Multiuser Time-Energy Entanglement Swapping Based on Dense Wavelength Division Multiplexed and Sum-Frequency Generation

Yuanhua Li,[1,2] Yiwen Huang,[1] Tong Xiang,[1] Yiyou Nie,[2] Minghuang Sang,[2] Luqi Yuan,[1] and Xianfeng Chen[1,*]
[1]State Key Laboratory of Advanced Optical Communication Systems and Networks, School of Physics and Astronomy, Shanghai Jiao Tong University, 800 Dongchuan Road, Shanghai 200240, China
[2]Department of Physics, Jiangxi Normal University, Nanchang 330022, China

(Received 28 June 2019; published 20 December 2019)

Perfect entanglement swapping, which can be realized without the postselection by using the nonlinear optical technology, provides an important way toward generating the large-scale quantum network. We explore an entanglement-swapping-based dense wavelength division multiplexed network in the experiment. Four users receive single quantum states at different wavelengths, and we perform a time-energy entanglement swapping operation based on the sum-frequency generation to make users fully connected in the network. The results show that the fidelity of the entangled state is larger than 90% and is independent of the number of users. Our Letter demonstrates the feasibility of a proposed multiuser network, and hence paves a route toward a variety of quantum applications, including entanglement-swapping-based quantum direct communication.

DOI: 10.1103/PhysRevLett.123.250505

Introduction.—A quantum network [1] is an important platform for applying quantum information and testing quantum theory. Each user in the quantum network not only shares the key by entanglement distribution to implement unconditional secure communication, but also performs the Bell-state measurement to realize the quantum information processing tasks, such as quantum teleportation [2] and entanglement swapping [3]. Entanglement swapping can establish the quantum entanglement between two independent photons without any interaction before [4], which is the basis for constructing a large-scale quantum network.

The Bell-state measurement is a core technology used to realize entanglement swapping [5]. However, due to the limitation in the linear optical Bell-state measurement, one can only identify two Bell states, while the other two Bell states cannot be resolved [6]. This makes this entanglement-swapping protocol useless in practice without postselection. Fortunately, it has been shown that the perfect entanglement swapping can be realized if the Bell-state measurement uses the sum-frequency generation (SFG) [7]. Furthermore, SFG between single photons at telecom wavelengths has been experimentally demonstrated [8–10], and one heralded entangled-photon pair in the visible wavelength regime with fidelity greater than 90% may be obtained in theory. However, the generated entangled-photon pair of the visible wavelength regime based on the SFG process cannot be used for the optical fiber network, and at the same time, the number of users of communication is also limited to only two users. Quantum networks extend the advantages of entanglement-swapping protocols without postselection by using the SFG for more than two remote users. The quantum entanglement of the telecommunications band can be established between any two users in the network, and different quantum information processing tasks, such as quantum direct communication, can be performed through the generated entanglement.

Here we present an entanglement-swapping-based dense wavelength division multiplexing (DWDM) network in which a single-photon source distributes N quantum states in the telecommunications band to N distant users. All distant users are in a fully connected graph by performing the Bell-state measurements based on SFG. In this Letter, we demonstrate the feasibility of our approach by using a single-photon source. The spectrum of the generated single-photon source is divided into four international telecommunication union (ITU) channels, where the frequency correlation of photons is built up via the DWDM, so two sets of time-energy entangled states are distributed to four users. Based on SFG between any two nonentangled photons, we can establish the entanglement between the other two independent photons. This makes four users a fully connected graph while allowing all pairs of users to generate the entanglement and the secure key using only a single-photon source. Our experiment requires no postselection and shows that the fidelity of the entangled state is only dependent on the transmission distance, which makes our proposal suitable for potentially building the large-scale quantum network.

Experiment.—Our design for the fully entanglement-swapping-based DWDM network is presented in Fig. 1. In our network, the quantum processor is used to generate a single-photon source and then distributes N single-photon states to N distant users by using one 100-GHz DWDM.

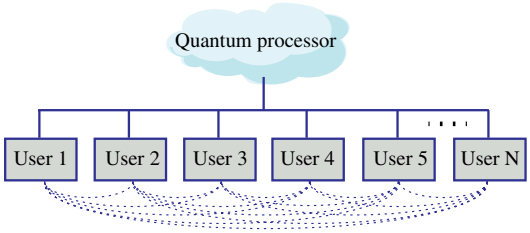

FIG. 1. The concept of the entanglement-swapping-based DWDM network.

Each user holds a photon at the specific wavelength and has one time-energy analysis and detection module. All users are in a fully connected network after performing the entanglement-swapping operations based on SFG. In order to implement a fully connected graph with N users, $N \times (N-1)/2$ links and $N/2$ entangled states are needed. Therefore, the desired single quantum state and single-photon detection system increases with a linear dependence as the number of users increases.

Next, we experimentally demonstrate the feasibility of our approach by using a single-photon source, which is multiplexed into four channels of different wavelengths. These four single quantum states are then distributed to four users (Alice, Bob, Chloe, and Dave). The experimental setup is shown in Fig. 2. Two frequency-correlated photon pairs from the spontaneous parametric down-conversion (SPDC) source are separated into four wavelength channels. Each user now receives one wavelength channel and can share a different entangled state with another user. To implement our network architecture, a 1551.72-nm (CH32) cw laser amplified by an erbium-doped fiber amplifier is used to generate a second harmonic generation (SHG) laser in the first temperature-stabilized periodically poled lithium niobate (PPLN) waveguide. A 780–1550-nm wavelength division multiplexing (WDM) is used to suppress the CH32 laser with an extinction ratio of about 180 dB. The generated SHG laser is used as a pump to create photon pairs through SPDC in the second PPLN waveguide. The generated photon pairs are separated from the SHG laser using another WDM with an extinction ratio of about 180 dB.

In this SPDC process, any set of correlated photon pairs are generated simultaneously, and the resulting processes are independent and equally probabilistic, while the resulting processes determined by the quasiphase matching conditions are independent and equally probabilistic [11,12]. In our experiment, the photon counts of the four channels (CH26, CH38, CH28, and CH36) are about the same. For the maximum output of the pump laser, the photon count of each channel is at the order of 10^8 per second. As shown in Fig. 2, the correlated photon pair (CH26, CH38) are sent to two unbalanced interferometers at Alice's and Dave's sites (Franson configuration) [13]. The correlated photons (CH26, CH38) can either travel along a short or a long path ($s_{A,D}$ or $l_{A,D}$). We consider the case when both photons exit the interferometer through the same path output, which gives the entangled state $|\Phi^+\rangle_{AD} = (1/\sqrt{2})(|ss\rangle + |ll\rangle)_{AD}$, where $|s\rangle$ and $|l\rangle$ are the quantum states of the correlated photon pair (CH26, CH38). In our experiment, Alice and Dave share one entangled state, and Bob and Chloe share the other entangled state. Fidelities of these two sets of entangled states are $(97.1 \pm 1.2)\%$ and $(97.5 \pm 1.5)\%$, respectively [14].

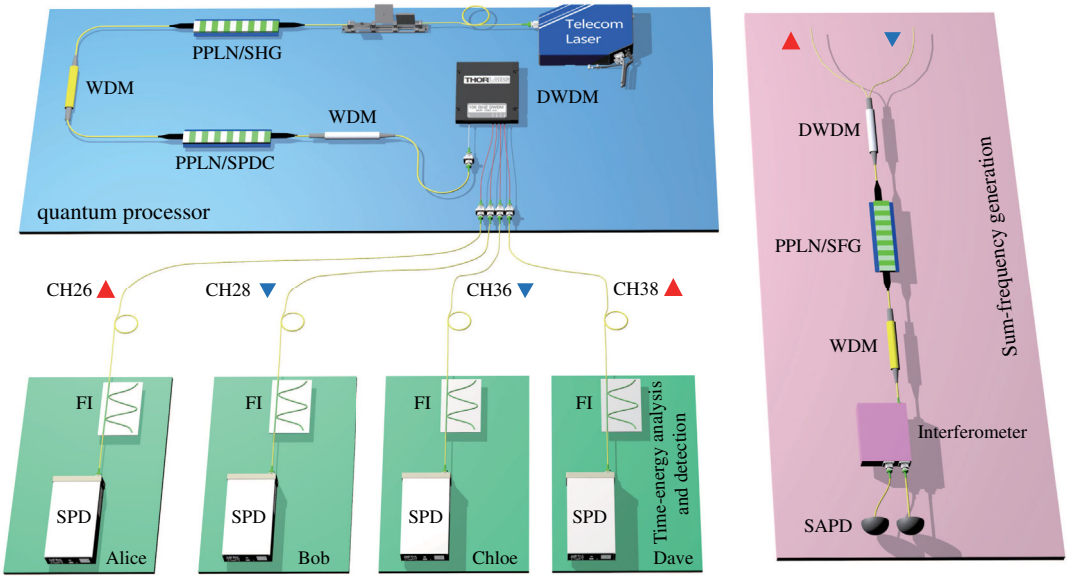

FIG. 2. Experimental setup. (Left) Entanglement-swapping-based DWDM quantum network. (Right) SFG between two nonentangled photons. Franson interferometry (FI). Single-photon detector (SPD) (quantum efficiency, $\eta_{\text{det}} = 10.0 \pm 0.2\%$; repetition frequency of gate, $f = 100$ MHz; width of gate, 1 ns; dark count probability per second, $D = 1 \times 10^{-6}$).

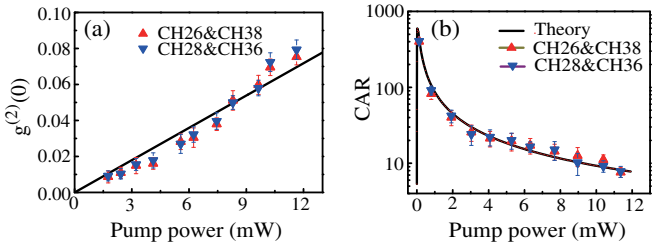

FIG. 3. (a) Measured $g^{(2)}(0)$ as a linear function of the pump power. (b) CAR for two sets of photon pairs generated by SPDC.

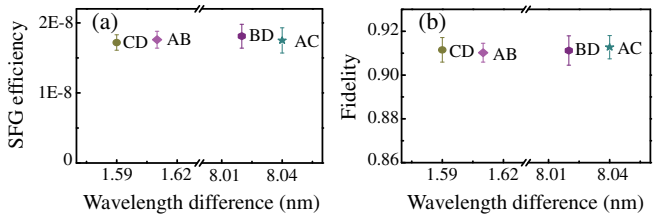

FIG. 4. (a) Measured SFG efficiency hat the two not-entangled photons are up-converted inside the PPLN waveguide. Each point is measured using the two ITU channels that link the corresponding users [Alice (A), Bob (B), Chloe (C), Dave (D)]. The integration time for each dot is 2 h. The x axis is the difference in wavelength between the channels of these two not-entangled photons. Dark counts of 3.2 Hz have been subtracted, and the total losses of about 4.9 dB have been taken into account. (b) The fidelity of the entangled state after entanglement swapping was obtained by the corresponding SFG efficiency.

To achieve the entanglement between users, two nonentangled photons are coupled simultaneously into the third PPLN waveguide (SH-50-PM-SM-2-2, SIQST) by a DWDM to create one SFG photon (Fig. 2, right). The peak SFG efficiency of the waveguide is about 15%. A stable temperature controller is used to keep the waveguide's temperature to maintain the quasi-phase-matching condition of the SFG process. The created SFG photon, after a high-isolation WDM (about 180 dB), is sent into a silicon avalanche photodiode (SAPD) (COUNT-100T-FC, ETSC Technologies Co.). The SAPD's detection efficiency is up to 60% at 775 nm and the dark count rate is about 23 Hz. The SFG photon is generated only when two photons are simultaneously coupled into the waveguide. The Bell-state measurement based on SFG needs to erase the which-path information by an unbalanced interferometer (Fig. 2, right). Two continuously generated SFG photons E and F can be used to distinguish all four Bell states. When the photons E and F pass through the interferometer, they are projected into the following four states: $|s\rangle_E$, $|l\rangle_E$, $|s\rangle_F$, and $|l\rangle_F$, which correspond to four Bell states, i.e., $|s\rangle_E \rightarrow |\Phi^+\rangle$, $|l\rangle_E \rightarrow |\Phi^-\rangle$, $|s\rangle_F \rightarrow |\Psi^+\rangle$, and $|l\rangle_F \rightarrow |\Psi^-\rangle$. Therefore, the entanglement-swapping process is completed once the SFG photons are detected. In our experiment, three temperature-stabilized 5-cm-long type-0 PPLN waveguides with a poling period of 19 μm are used.

Results and discussions.—To verify the single-photon nature of our SPDC source, we measured the second-order correlation function $g^{(2)}(0)$ and the coincidence-to-accidental ratio (CAR), as shown in Fig. 3. First, we measured $g^{(2)}(0)$ of the two sets of signal photons CH36 and CH38, where idler photons of CH28 and CH26 as trigger signals are used, respectively. Then, the CAR for two sets of photon pairs was measured, as shown in Fig. 3(b).

In theory, $g^{(2)}(0)$ and CAR can be expressed as [12]

$$g^{(2)}(0) \approx \triangle t \eta_p P_p, \tag{1}$$

$$\mathrm{CAR} = \frac{C\eta_s\eta_i}{(C+\eta_s D_i)(C+\eta_i D_s)}, \tag{2}$$

where $\triangle t$ is the duration of the detector gate, η_p is the photon pair creation efficiency of SPDC, P_p is the pump power, and C is the coincidence count per detection gate. η_s and η_i are the transmission efficiencies of signal and idler channels. D_s and D_i are the dark count rates per gate. In our Letter, $\triangle t = 1\,\mathrm{ns}$, $\eta_p = 4 \times 10^{-9}$, and $D_s = D_i = 1 \times 10^{-6}$. η_s and η_i were independently measured [14]. Figure 3(a) shows that two sets of $g^{(2)}(0)$ are proportional to the pump power generated by SHG, and Fig. 3(b) gives the relationship between the pump power and CAR. From the experimental results, all wavelength channels exhibit the same single-photon nature. Furthermore, our experimental measurements are in agreement with the theoretical results.

To complete the entanglement swapping, we need to perform a Bell-state measurement on two nonentangled photons using SFG. In our experiment, four sets of wavelength channels are not entangled, i.e., CH36 and CH38, CH26 and CH28, CH28 and CH38, and CH26 and CH36. As shown in Fig. 4(a), the four sets of SFG efficiencies were independently measured before the multiplexing of four channels to each user, where the pump power is kept at 12 mW. In this case, we can obtain $g^{(2)}(0) = 0.08$ and $\mathrm{CAR} = 10$, and hence, the characteristics of the single photon and the good signal-to-noise ratio are guaranteed in our experiment (Fig. 3).

It is shown that the theoretical SFG efficiency is given by $\eta'_{\mathrm{SFG}} = (\xi \mathrm{Ł}^2 h\nu\triangle\nu)/\mathrm{TBP}$, where ξ denotes the measured PPLN waveguide peak efficiency, L is the PPLN waveguide length, $\triangle\nu$ denotes the pump photon bandwidth, and TBP represents the time-bandwidth product. Here we consider that $\xi = 15\%/(\mathrm{W\,cm^2})$, $\triangle\nu = 100$ GHz, and $\mathrm{TBP} = 0.66$. Thus, the theoretical SFG efficiency is $\eta'_{\mathrm{SFG}} = 2 \times 10^{-8}$. One notices that the experimental SFG efficiencies are in agreement with the theoretical result.

According to the proposed theory [7], we can obtain the equation for the fidelity, which is given by $P = \frac{1}{18}\eta_c^2\eta^2\eta_{\mathrm{SFG}}(1-F)^2(2-F)$, where P is the success probability for the fourfold coincidence, η_c is the overall coupling efficiency, and η represents the single-photon

detection efficiency. When $P=3\times10^{-12}$ and $\eta_c=\eta=\sqrt{0.6}$, we can obtain the fidelity of the generated entangled state based on our experimental SFG efficiency, as shown in Fig. 4(b).

In our experiment, there are two kinds of methods for observing the fidelity of an entangled state generated by the entanglement swapping. The first method is to detect single photons in the other two channels via two ultralow temperature superconducting nanowire single-photon detectors, and then use SFG photons as a trigger signal to measure the fidelity of the generated entangled state. The other method is to measure directly the fidelity by using two-photon interference fringe [6]. Here we chose the latter method. We show that the fidelity of the shared entangled state has not been changed by the entanglement-swapping operation [17]. Therefore, we can obtain the fidelity of the generated entangled state by measuring the fidelity of the previously entangled state before performing the entanglement swapping [14].

Here we assume that Alice and Bob establish the entanglement, and the corresponding SFG efficiency of $(1.72\pm0.11)\times10^{-8}$ was measured (Fig. 4). Obviously, the Bell-state measurement of the two not-entangled photons (CH36 and CH38) based on the SFG process leads to an increase in the total loss of one of the entangled photons to about 77.64 dB. Therefore, we attenuate the CH26 and CH38 channels by 38.82 dB per channel using two variable optical attenuators and then measure the fidelity of the time-energy entangled state. It is been demonstrated that the measured fidelity F_{AD}^{EXP} is equal to the fidelity of the generated entangled state F_{AB}^{EXP} [14].

To measure the fidelity, we use the planar lightwave circuit interferometer with 1-ns relative delay in our experiment (Fig. 2). The two-photon interference fringes for time-energy entangled channels (CH26 and CH38) can be measured. The theoretical expression for the visibility is [18]

$$V=\frac{n\alpha_s\alpha_i}{n\alpha_s\alpha_i+2(n\alpha_s+2D_s)(n\alpha_i+2D_i)}, \tag{3}$$

where $\alpha_{s,i}$ are the losses from signal and idler channels (CH26 and CH38), respectively, $D_{s,i}$ are dark count probability per second with $D_s=D_i=1\times10^{-6}$, and n is a mean photon pair number per detection gate. In our experiment, the pump power is set to generate the mean photon pair number $n=0.04$ per detection gate. We obtain average visibility of $V_{AB}^{\mathrm{EXP}}=(87.2\pm4.8)\%$ for time-energy entanglement (Fig. 5). This result agrees closely with the theoretical predication, $V_{AB}^{\mathrm{TH}}=84.8\%$ from above Eq. (3).

According to the equation $F_{AB}=0.75V_{AB}+0.25$ given by [19], we can obtain the fidelity of $F_{AB}^{\mathrm{EXP}}=(90.4\pm3.6)\%$. Based on the corresponding SFG efficiency [Fig. 4(a)], we obtained the fidelity of the other three sets of entangled states, i.e., $F_{CD}^{\mathrm{EXP}}=(91.2\pm2.8)\%$, $F_{BD}^{\mathrm{EXP}}=(90.8\pm3.2)\%$, and $F_{AC}^{\mathrm{EXP}}=(91.3\pm3.7)\%$ (Fig. 5), which is in agreement with the results [Fig. 4(b)]. Our results show that we have successfully completed the entanglement swapping with a fidelity greater than 90% using SFG.

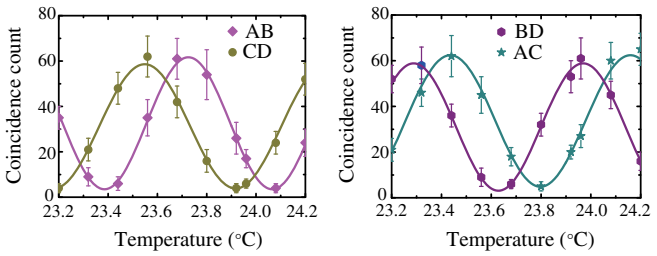

FIG. 5. Two-photon interference fringe is obtained by the corresponding SFG efficiency. Coincidence count is shown for the channel pair CH26-CH38. The x axis is the temperature of the interferometer in the CH26, and CH38's interferometer temperature stays unchanged. The measuring time for each dot is 3000 s.

In our network, the single-photon source can cover more than 40 ITU channels (from CH12 to CH52), and all channels have virtually identical efficiencies. Our results show that, when the difference in wavelength between two nonentangled photons simultaneously coupled into the third waveguide is no more than 21 nm, the resulting SFG efficiency is almost the same. In order to ensure that the fidelity of the generated entangled state after entanglement swapping is larger than 90%, only 26 channels (from CH18 to CH45, except CH32) can be used in our network, which gives the maximum number of users allowed in our network.

Compared with other proposed full connected quantum networks [20,21], our proposed network has the following five characteristics. First, the time-energy entanglement in our Letter does not require one to control the polarizations of photons, which is more suitable for fiber-based quantum key distribution (QKD) systems. Second, the process for establishing entanglements is deterministic when the SFG photons are detected, which leads to a quantum direct communication process. Third, the number of entangled states distributed increases linearly with the increase of the number of users, and the quantum bit error rate in the distribution process is only related to the transmission distance. Fourth, the fidelity of the quantum entanglement shared by each user is only related to the transmission distance and is independent of the number of users in the network. Finally, our network does not require single-photon wavelength conversion [22] and frequency shift between all users, making our network more suitable for constructing a large fiber-based quantum network, and has also potential applications in multidimensional QKD [23]. Our experiment connects any two users after the entanglement-swapping operation with the destructive measurement of all other nodes in the network.

Summary.—We have successfully demonstrated the feasibility of our entanglement-swapping-based DWDM

network. Each user in the network only receives the photon at a specific wavelength. In our experiment, we can establish the entanglement between any two nonentangled states based on SFG. Furthermore, our network architecture does not require any trusted nodes, and all users can transfer the quantum information and share secure keys by establishing the entanglement. In addition, we notice that our network can achieve a 200-km entanglement distribution in which the coincidence count is more than 72 bits/h. Moreover, if a high-performance SPD in Ref. [24] is used, it is possible to increase the coincidence count up to ~6 kbits/h. Because of the scalability of our quantum network, it can be used for real quantum systems, such as point-to-point quantum direct communication.

This work is supported in part by the National Key Research and Development Program of China (Grant No. 2017YFA0303700), National Natural Science Foundation of China (Grant No. 11734011, No. 11804135, No. 11764021, and No. 61765008), and The Foundation for Development of Science and Technology of Shanghai (Grant No. 17JC1400400).

*xfchen@sjtu.edu.cn

[1] S.-K. Liao, W.-Q. Cai, J. Handsteiner, B. Liu, J. Yin, L. Zhang, D. Rauch, M. Fink, J.-G. Ren, W.-Y. Liu *et al.*, Phys. Rev. Lett. **120**, 030501 (2018).
[2] Q.-C. Sun, Y.-L. Mao, S.-J. Chen, W. Zhang, Y.-F. Jiang, Y.-B. Zhang, W.-J. Zhang, S. Miki, T. Yamashita, H. Terai *et al.*, Nat. Photonics **10**, 671 (2016).
[3] P. Xu, H.-L. Yong, L.-K. Chen, C. Liu, T. Xiang, X.-C. Yao, H. Lu, Z.-D. Li, N.-L. Liu, L. Li *et al.*, Phys. Rev. Lett. **119**, 170502 (2017).
[4] J.-W. Pan, D. Bouwmeester, H. Weinfurter, and A. Zeilinger, Phys. Rev. Lett. **80**, 3891 (1998).
[5] X.-s. Ma, S. Zotter, J. Kofler, R. Ursin, T. Jennewein, Č. Brukner, and A. Zeilinger, Nat. Phys. **8**, 479 (2012).
[6] Q.-C. Sun, Y.-F. Jiang, Y.-L. Mao, L.-X. You, W. Zhang, W.-J. Zhang, X. Jiang, T.-Y. Chen, H. Li, Y.-D. Huang *et al.*, Optica **4**, 1214 (2017).
[7] N. Sangouard, B. Sanguinetti, N. Curtz, N. Gisin, R. Thew, and H. Zbinden, Phys. Rev. Lett. **106**, 120403 (2011).
[8] T. Guerreiro, A. Martin, B. Sanguinetti, J. S. Pelc, C. Langrock, M. M. Fejer, N. Gisin, H. Zbinden, N. Sangouard, and R. T. Thew, Phys. Rev. Lett. **113**, 173601 (2014).
[9] T. Guerreiro, E. Pomarico, B. Sanguinetti, N. Sangouard, J. Pelc, C. Langrock, M. Fejer, H. Zbinden, R. T. Thew, and N. Gisin, Nat. Commun. **4**, 2324 (2013).
[10] Y. Li, T. Xiang, Y. Nie, M. Sang, and X. Chen, Photonics Res. **5**, 324 (2017).
[11] F. Lenzini, A. N. Poddubny, J. Titchener, P. Fisher, A. Boes, S. Kasture, B. Haylock, M. Villa, A. Mitchell, A. S. Solntsev *et al.*, Light **7**, 17143 (2018).
[12] T. Xiang, Y. Li, Y. Zheng, and X. Chen, Opt. Express **25**, 12493 (2017).
[13] J. D. Franson, Phys. Rev. Lett. **62**, 2205 (1989).
[14] See Supplemental Material at http://link.aps.org/supplemental/10.1103/PhysRevLett.123.250505 for transmission efficiency per ITU channel, the method of analyzing the time-energy entangled state, and proof of fidelities of entanglement swapping in noiseless and noisy environments, which includes Refs. [15,16].
[15] C. H. Bennett, G. Brassard, S. Popescu, B. Schumacher, J. A. Smolin, and W. K. Wootters, Phys. Rev. Lett. **76**, 722 (1996).
[16] R. Fortes and G. Rigolin, Phys. Rev. A **92**, 012338 (2015).
[17] Z.-j. Zhang and Z.-x. Man, Phys. Rev. A **72**, 022303 (2005).
[18] J. Dynes, H. Takesue, Z. Yuan, A. Sharpe, K. Harada, T. Honjo, H. Kamada, O. Tadanaga, Y. Nishida, M. Asobe *et al.*, Opt. Express **17**, 11440 (2009).
[19] H. de Riedmatten, I. Marcikic, J. A. W. van Houwelingen, W. Tittel, H. Zbinden, and N. Gisin, Phys. Rev. A **71**, 050302(R) (2005).
[20] S. Wengerowsky, S. K. Joshi, F. Steinlechner, H. Hübel, and R. Ursin, Nature (London) **564**, 225 (2018).
[21] I. Herbauts, B. Blauensteiner, A. Poppe, T. Jennewein, and H. Huebel, Opt. Express **21**, 29013 (2013).
[22] T. Xiang, Q.-C. Sun, Y. Li, Y. Zheng, and X. Chen, Phys. Rev. A **97**, 063810 (2018).
[23] J. Mower, Z. Zhang, P. Desjardins, C. Lee, J. H. Shapiro, and D. Englund, Phys. Rev. A **87**, 062322 (2013).
[24] F. Marsili, V. B. Verma, J. A. Stern, S. Harrington, A. E. Lita, T. Gerrits, I. Vayshenker, B. Baek, M. D. Shaw, R. P. Mirin *et al.*, Nat. Photonics **7**, 210 (2013).